



THE ELECTROCHEMICAL BEHAVIOUR OF SOME COMPOSITE COATINGS WITH DIFFERENT ADDITIVES OBTAINED BY ELECTRODEPOSITION ON METALLIC SUBSTRATE

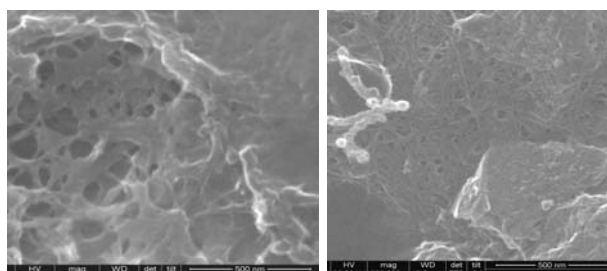
Florina BRANZOI,^{a*} Zoia PAHOM^b and Viorel BRANZOI^b

^a Institute of Physical Chemistry "Ilie Murgulescu" 202 Splaiul Independenței, 060021 Bucharest, Roumania

^b University Politehnica of Bucharest, Faculty of Applied Chemistry and Materials Science, Department of Inorganic Chemistry, Physical Chemistry and Electrochemistry, 132 Calea Griviței, 010737 Bucharest, Roumania

Received June 15, 2017

Nanocomposite films of polyaniline and functionalized carbon nanotubes (FCNTs) with different additives have been electrochemically deposited from synthesis solutions such that constituents were deposited simultaneously onto metallic substrate. Cyclic voltammetry (CV) and electrochemical impedance spectroscopy (EIS) techniques established that these composite films had electrochemical like response rates to pure polymeric films however a reduced resistance and much improved mechanical integrity. The morphology of composite films has been investigated by scanning electron microscopy (SEM). The negatively charged functionalized carbon nanotubes (CNTsF) and additives utilized as anionic dopant through the electropolymerization to obtain polymer/CNTsF composite films. The electrochemical and physical properties like specific electrochemical capacitance of the composite films is a meaningful bigger value than that for pure polymer films obtained likewise. The additives substances used were: cetyl benzyl dimethyl ammonium chloride (CBDACL) and KClO_3 . Using these composite films, the modified electrodes with enhanced characteristics were achieved.



INTRODUCTION

Many researches have investigated to combine carbon nanotubes and conducting polymers for application as modified electrodes in various practices through conductive and high-strength composites, energy storage and energy conversion devices, batteries, capacitors, corrosion protection, coatings, sensor applications, field emission displays and radiation sources, hydrogen storage media etc.¹⁻⁵

Conducting polymers can be doped and de-doped rapidly to high charge density and as a result are potential active materials for use in various electrochemical applications. Conducting polymers are also intriguing molecular structures because

their ability to dramatically change properties when stimulated by an electric signal. These materials offer exciting prospects for a wide range of new devices as membranes, artificial muscles, solar cells, batteries, capacitors, corrosion protection coatings or sensor applications.^{4-9, 26} Thus an important application is the fabrication of modified electrodes. For this consideration, the nanocomposite materials based on the functionalized carbon nanotubes, conducting polymers and different anionic dopants were grown electrochemically onto a platinum substrate from a synthesis solution.

Carbon nanotubes (CNTs), as one of the most important carbon materials, have attracted a great interest over the recent years, as an effect of their

* Corresponding author: fbrinzoi@chimfiz.icf.ro

special properties and wide domain of applications. Their very high mechanical resilience, nanometer size, high accessibility surface area, high electrical conductivity, chemical and mechanical characteristics are especially significant for various practice such as in nanoelectronics, biosensors, supercapacitors and so on.^{2,5-19} All the obtained composites showed improved mechanical integrity, higher electronic and ionic conductivity and exhibited larger electrode specific capacitance than the polymer alone. The negatively charged FCNTs served as anionic dopant during the electropolymerization to synthesize CP/FCNTs composite films.¹⁴⁻²⁵ The intensive interaction between the most delocalized π electron of CNTs and the π electron corresponded with the structure of the polymers framework increases the electron / orifice assignment between CNTs and conducting polymers.^{9,10,25}

This research is a continuation of previous work on the synthesis and electrochemical characterized of the composite films doped with some functionalized single-walled carbon nanotubes and some additives that have been deposited on the platinum substrate by electrochemical method.

In this paper we presented an electrochemical synthesis of nanocomposite films from conducting polymers aniline, functionalized carbon nanotubes (SWCNTsF with carboxylic acid) and different additives: cetyl benzyl dimethyl ammonium chloride (CBDACl) and KClO_3 . The electrochemical characterization of these nanocomposites has been done by cyclic voltammetry, electrochemical impedance spectroscopy and scanning electron microscopy. The synthetic, morphological and electrochemical properties of nanocomposite materials type CP/FCNTs / dopants were compared.

EXPERIMENTAL

The electrochemical polymerization and characterization were realized by using a single-compartment cell with the conventional three electrodes set up at room temperature. The electrochemical cell was connected to a VoltaLab potentiostat coupled to a PC running VoltaMaster software. A saturated calomel electrode (SCE) was used as the reference electrode and a platinum plate as an auxiliary electrode. The working electrode was a platinum disk with a surface area of 0.5 cm^2 . All chemicals were reagent grade and used as received without further purification. In this paper were used aniline (99.5% Fluka), H_2SO_4 (96% Merck), cetyl benzyl dimethyl ammonium chloride (98% Fluka), KClO_3 (96% Fluka) and single-walled carbon nanotubes functionalized with carboxylic acid (FSWCNTs) were the commercial product from Sigma-Aldrich with the following characteristics: 80-90% carbon basis, $D \times L$ 2-10 nm \times 0.5-2 μm , bundle dimensions. All the solutions were prepared with double distilled water.

Preparation of modified electrode

Prior each electrochemical experiment the surface of the platinum electrode has been polished with 0.3, 0.01 and 0.05 μm alumina powders and rinsed in double distilled water and ethanol. The prepared electrodes were dried and used for modification. Experimental methods were described previously.²⁻⁵ Nanocomposite films of CPs/FSWCNTs have been obtained by electrochemical polymerization from a synthesis solution containing the functionalized carbon nanotubes (FSWCNTs) and the corresponding monomer (aniline). FSWCNTs were used in this paper namely: single wall carbon nanotubes (SWCNTs) functionalized with carboxylic acid. The negatively charged SWCNTs-COOH in solution acted as sole supporting electrolyte and additives for the PANI depositions. For this fact CNTsF are wrapped in polymers during the electropolymerization process in the form of counter ions or dopants.

Thus, PANI/CNTsF/additives composite films were obtained from an synthesis solution containing 0.2 mol/L aniline + 0.25 mol/L H_2SO_4 + 0.5 mg/SCNTsF and 0.2 M various additives (cetyl benzyl dimethyl ammonium chloride (CBDACl) and KClO_3) by cyclic voltammetry in the potential scanning range of -250 to +900 mV at a sweep rate of 10 mV/s and for a cycles number of 10. The pure PANI films were prepared from an aqueous solution of 0.2 mol/L aniline + 0.25 mol/L H_2SO_4 , without adding CNTsF and additives.

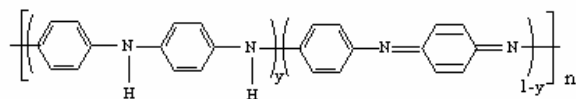
Characterization of the modified electrodes

Cyclic voltammetry and electrochemical impedance spectroscopy have been utilized to investigate the physical and electrochemical properties of the composite films.

The electrochemical characterization of the PANI-CNTsF-additives composite films has been performed in 0.25 mol/L H_2SO_4 aqueous solution by cyclic voltammetry in the potential scanning domain of -250 to +900 mV at a sweep rate of 50mV/s and for a cycles number of 50. The electrochemical impedance spectroscopy experiments were realized using a VoltaLab 40 potentiostat /galvanostat with EIS dynamic in the frequency range of 100 kHz \div 1 mHz with an AC wave of 5 mV (peak-to-peak) overlaid on a DC bias potential and the impedance data were obtained at a rate of 10 points per decade change in frequency. All tests have been performed at 25° C under atmospheric oxygen without agitation.

RESULTS AND DISCUSSION

In the first stage, the PANI/Pt coating has been also electrodeposited onto electrode surface (platinum) by electrochemical polymerization from a synthesis solutions containing 0.2 mol/L aniline and 0.25 M H_2SO_4 as supporting electrolyte (see figure 1 Inset). The obtained the PANI/Pt /Pt film was presented in previous work.²⁵ It can be said that polyaniline can exist in three different oxidation states such as leucoemeraldine (fully reduced form $y = 1$), emeraldine (partially oxidized form $y = 0.5$) and pernigraniline (fully oxidized form $y = 0$) as shown in the following scheme:



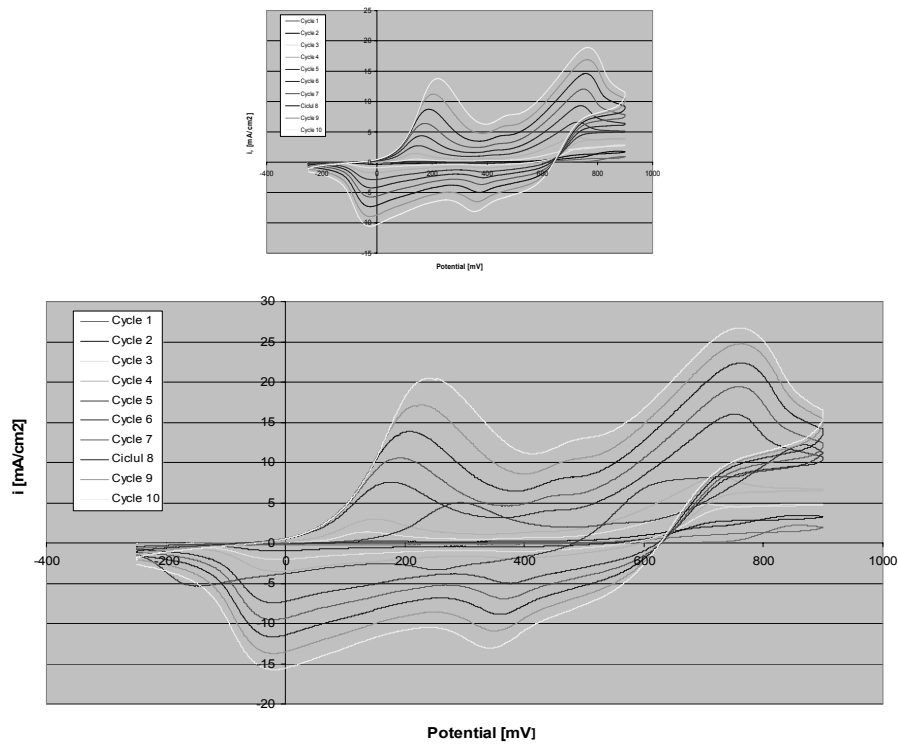


Fig. 1 – Polymerization cyclic voltammograms of aniline + SWCNTs- COOH in 0.25 M H_2SO_4 aqueous. solution. Inset electropolymerization PANI/Pt at 25°C.

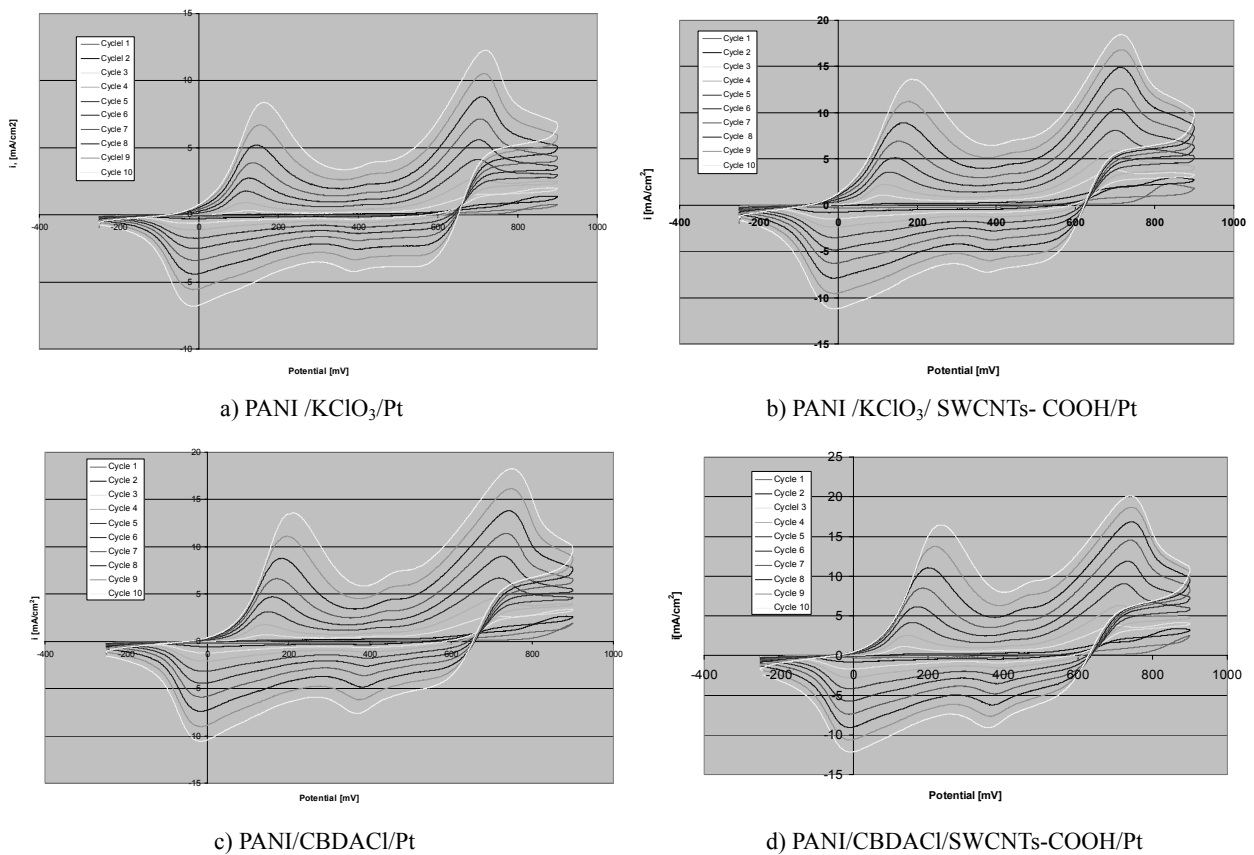


Fig. 2 – Polymerization cyclic voltammograms of a) PANI/ $KClO_3$ /Pt; b) PANI/ $KClO_3$ /SWCNTs- COOH/Pt; c) PANI/cetyl benzyl dimethyl ammonium chloride/Pt; d) PANI/cetyl benzyl dimethyl ammonium chloride /SWCNTs- COOH/Pt in 0.25 M H_2SO_4 aqueous at 25°C.

The three polyaniline oxidation forms are indicated to the three anodic oxidation peaks while the three polyaniline (PANI) reduction states are shown by the three reduction peaks from the cathodic branch of cyclic voltammograms (figure 1-inset). These states of polyaniline are influenced on the applied potential.

Composite films of polyaniline-and functionalized, single-walled carbon nanotubes with polycarboxylic acid (PANI/SWCNTs-COOH) were fabricated by a simple oxidative electropolymerization method. These composite films were electrodeposited on a platinum working electrode using a classical system with three electrodes. The obtained cyclic voltammograms for PANI/SWCNTs-COOH /Pt are given in Figure 1 and have the same shapes with those obtained for PANI/Pt modified electrode cycled in the same conditions, but in this case the anodic peaks are much higher and in the main the anodic and cathodic currents are much greater than those for PANI film. From figure 1 and table 1 it can be observed that the current is increasing upon continuous cycling, being indicative for a conductive film formation. This situation can be assigned considering that, FSWCNTs (in our case SWCNTs-COOH) are negatively charged and they can function as doped anions and consequently, the conductivity of PANI/FSWCNTs composite film increases.

The PANI/SWCNTs-COOH/dopant films were achieved on the platinum substrate in a synthesis solution of 0.2 mol/PANI + 0.5 mg/L SWCNTs-COOH + 0.2 mol/L dopant substance in 0.25 M H₂SO₄ by cyclic voltammetry in the scanning potential range of -250 to +900 mV at a scan rate of 10 mV/s and for 10 cycles. The additives substances used were: cetyl benzyl dimethyl ammonium chloride (CDMACl) and KClO₃. In the presence of additives CDMACl and KClO₃ with and without SWCNTs-COOH, see figure 2a-d, it is observed that the current response of doped PANI films increases with addition of the additive with SWCNTs-COOH, especially when the cetyl benzyl dimethyl ammonium chloride is added. In this situation from figure 2, the cyclic voltammograms show greater and larger oxidation and reduction peaks and in general the anodic and cathodic currents are much higher than the case from figure 1 inset. Moreover, the current increases with

continuous cycling in the potential domain as seen in figure 1-2. This case can be explained considering the fact that SWCNTs-COOH/dopant is negatively charged and they are able to function as anions and consequently, the conductivity of PANI/SWCNTs-COOH/additive composite film is higher.

Examining in comparison the cyclic voltammograms of PANI, PANI/SWCNTs-COOH and PANI/SWCNTs-COOH/additive composite film, (figures 1, 2 and tables 1-3), clearly were indicated differences. Also, the voltamogram curves have the same shape in all cases, but the current intensities are lower in situation of pure PANI than with respect to nanocomposite/dopant and they increase upon continuous cycling as it can be seen from voltammograms from figures 1-2 and tables 1-3. The PANI/SWCNTs-COOH composites presents higher currents (20.42 mA/cm²) than PANI films (12.48 mA/cm²), which interprets into greater capacitance. Hence, the PANI/SWCNTs-COOH presenting more a porous composition for ion mobility a greater and potential-separate electronic conductivity by the adsorbed SWCNTs film, can explicate the difference in current from PANI and PANI/FSWCNTs-COOH/dopant. Therefore, in fully reduced state the PANI chains get neutral and the negative charge of immobile CNTs and ions of dopant (cetyl benzyl dimethyl ammonium chloride and KClO₃) are equalized of the cations with small dimension from the supporting electrolyte solution. The exhibited data show a quicker kinetics in the composite, that can be assigned to the higher electronic conductivity of the FSWCNTs network and dopant. Consequently the redox reactions that occur in nanocomposite film are more complex and more intensive than the ones in the pure PANI/ film.

The electrochemical behaviour of the PANI, PANI/SWCNTs-COOH, PANI/SWCNTs-COOH/dopant composite films deposited electrochemically from synthesis solution in the absence and presence of additives: cetyl benzyl dimethyl ammonium chloride and KClO₃ has been characterized further using cyclic voltammetry. The electrochemical characteristics of achieved PANI/Pt film was studied in the cycling solutions of 0.25M H₂SO₄ (see figure 3 Inset) and it was presented in previous work.

Table 1

Electrochemical parameters from polymerization curves achieved at the formation of PANI/SWCNTs-COOH composite film

Cycles	Anodic peaks						Cathodic peaks					
	Ea1, mV	ia1, mA/cm ²	Ea2, mV	ia2, mA/cm ²	Ea3, mV	ia3, mA/cm ²	Ec1, mV	ic1, mA/cm ²	Ec2, mV	ic2, mA/cm ²	Ec3, mV	ic3, mA/cm ²
Cycle 1					865	1.48789					358	-0.19688
Cycle 2	153	0.223437	413	0.271485	865	3.46368	-9	-0.95977	380	0.232813	544	0.539454
Cycle 3	136	1.36094	418	0.690234	714	4.78516	-12	-2.02851	387	-1.11172	565	-0.1043
Cycle 4	149	2.9711	429	1.40039	725	8.30742	-16	-3.51132	388	-2.04766	527	-0.9832
Cycle 5	166	5.01406	431	2.49062	741	12.2047	-19	-5.36132	385	-3.34961	567	-1.13359
Cycle 6	177	7.58399	444	4.0336	753	16.0235	-25	-7.42969	371	-5.00781	570	-1.85548
Cycle 7	190	10.5703	457	5.94531	759	19.4454	-24	-9.55469	365	-6.94922	571	-2.65625
Cycle 8	209	13.8555	467	8.07422	764	22.3711	-19	-11.6836	360	-8.87891	565	-3.59375
Cycle 9	224	17.2226	481	10.4141	767	24.7656	-18	-13.7461	349	-10.9258	531	-5.67188
Cycle10	240	20.4766	497	12.9844	763	26.7226	-15	-15.7422	340	-13.0586	518	-7.16406

Table 2

Electrochemical parameters from polymerization curves achieved at the formation of PANI/KClO₃/SWCNTs-COOH composite film

Cycles	Anodic peaks						Cathodic peaks					
	Ea1, mV	ia1, mA/cm ²	Ea2, mV	ia2, mA/cm ²	Ea3, mV	ia3, mA/cm ²	Ec1, mV	ic1, mA/cm ²	Ec2, mV	ic2, mA/cm ²	Ec3, mV	ic3, mA/cm ²
Cycle 1					853	1.84766					405	-0.16016
Cycle 2	139	0.171875	442	0.284375	864	2.68828	-33	-0.67891	384	-0.37344	572	0.117969
Cycle 3	118	0.88125	410	0.507422	693	3.20156	-13	-1.27344	393	-0.67383	520	-0.38164
Cycle 4	115	1.9082	412	0.872656	696	4.93399	-2	-2.01329	402	-1.0793	541	-0.68008
Cycle 5	127	3.04141	399	1.30079	697	6.64766	-6	-2.91524	398	-1.60664	557	-1.1207
Cycle 6	137	4.34141	424	1.98125	703	8.45313	-1	-3.96954	396	-2.25938	559	-1.70391
Cycle 7	151	5.85704	433	2.76016	706	10.2547	-1	-5.15039	398	-3.01914	547	-2.5
Cycle 8	159	7.58125	441	3.66485	709	11.9766	-3	-6.41289	385	-3.8707	543	-3.29882
Cycle 9	169	9.51055	449	4.64844	709	13.5274	-2	-7.70704	384	-4.78906	537	-4.16016
Cycle10	184	11.5898	457	5.75	711	14.9101	0	-9.08204	387	-5.80079	530	-5.07031

Table 3

Electrochemical parameters from polymerization curves achieved at the formation of PANI/ cetyl benzyl dimethyl ammonium chloride SWCNTs-COOH composite film

Cycles	Anodic peaks						Cathodic peaks					
	Ea1, mV	ia1, mA/cm ²	Ea2, mV	ia2, mA/cm ²	Ea3, mV	ia3, mA/cm ²	Ec1, mV	ic1, mA/cm ²	Ec2, mV	ic2, mA/cm ²	Ec3, mV	ic3, mA/cm ²
Cycle 1												
Cycle 2	136	0.157422	408	0.33086			-7	-0.83633	394	-0.46445		
Cycle 3	138	1.16055	409	0.666798	702	3.82344	-10	-1.70586	393	-0.92539		
Cycle 4	143	2.55039	426	1.22617	712	6.31172	-12	-2.81993	390	-1.57735		
Cycle 5	157	4.17969	430	2.01172	724	9.04336	-12	-4.20274	390	-2.46211		
Cycle 6	169	6.15781	433	3.03281	734	11.882	-13	-5.75938	388	-3.55079		
Cycle 7	187	8.48594	451	4.3961	739	14.5351	-13	-7.41016	376	-4.85156		
Cycle 8	199	11.0547	462	5.95704	740	16.8437	-14	-9.05469	371	-6.23048		
Cycle 9	216	13.7461	474	7.65625	741	18.6641	-14	-10.6602	363	-7.66016		
Cycle10	231	16.4375	494	9.47656	744	20.1016	-17	-12.1211	356	-9.11719		

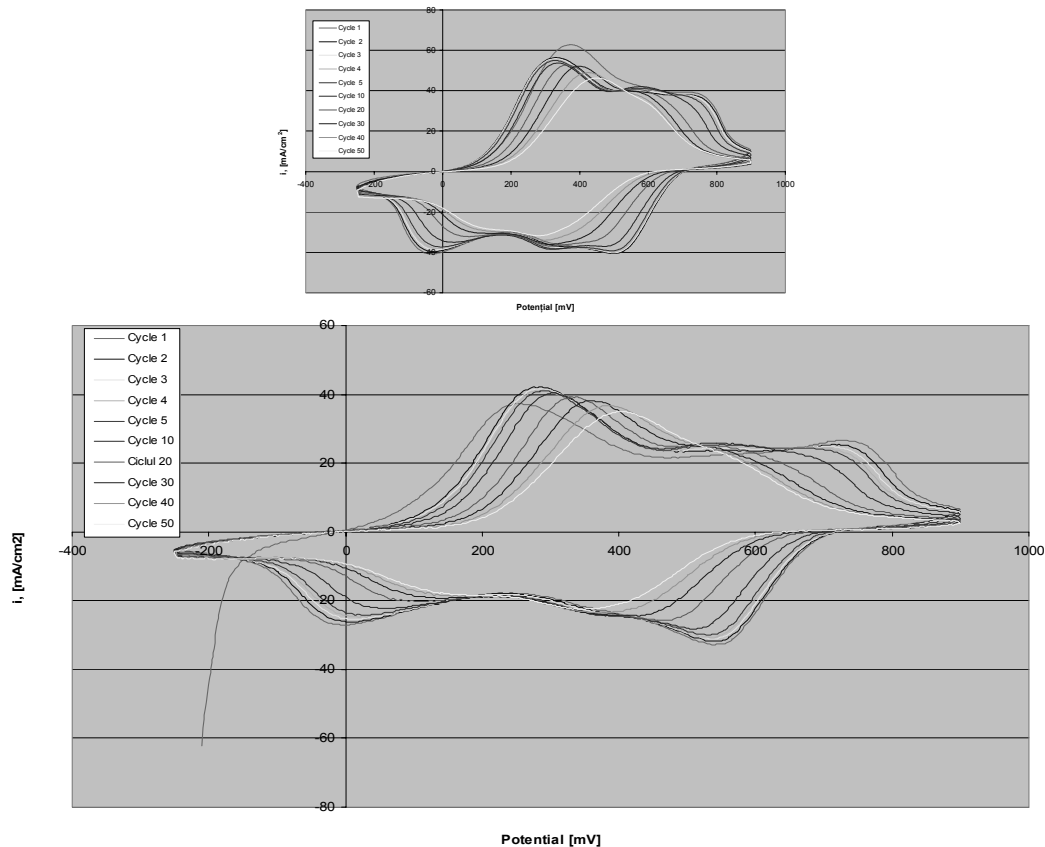


Fig. 3 – Cyclic voltammograms of PANI/SWCNTsF composite film in 0.25 M H₂SO₄ cycling solution (monomer free) at 25°C. Inset PANI/Pt.

Figures 3-5 represent the cyclic voltammograms of PANI/SWCNTs-COOH, PANI/SWCNTs-COOH/additive (cetyl benzyl dimethyl ammonium chloride and KClO₃) composite films accomplished in aqueous solution of 0.25M H₂SO₄ in wide potential domain to explore all eventual electrochemical properties of this composite film in electrolyte. The modified electrode type PANI/SWCNTs-COOH/dopant/Pt was achieved on the potential domain from -250 up to 900 mV with a sweep rate of 50mV/s and for a cycles number of 50, see figures 3-5. These films can be cycled repeatedly between the conducting (oxidized) and insulating (neutral) state without significant decomposition of the material, which is consistent with the results reported in the literature.^{9,10,16,17,23-26} For the cyclic voltammograms to exhibit better capacitive features (*e.g.* a rectangular shape), the potential ranges should be chosen to avoid the polymer becoming undoped and thus insulating, at very negative potentials and overoxidized at too positive potentials. As can be seen, the curves of these composite films have nearly rectangular shape, which is typical of the pure capacitive behaviour of the tested object.

The first redox peak is commonly ascribed to the electron transfer from/to the PANI film. In sequence to compensate the charge of the PANI film, anion doping/de-doping of the PANI film appears. The second redox peak assigned to a deprotonation and protonation process. In addition, the proton/cation shift the anion is also excluded from the PANI film through deprotonation. A small peak at assigned 400 mV is presumably as a result to a side reaction in the PANI film. At the negative and positive ends of the potential scan, the pure PANI film transformed into its non-conducting states. The same appeared to the PANI-CNTs-COOH/dopant composite film. The capacitance of PANI/CNTsF and PANI/CNTsFs/dopant is larger than that of the pure polymeric PANI films since the composition of CNTsF achieves the doping ions enters into/eject from PANI/CNTsF composite films more readily. Also, the PANI-CNTs-COOH and PANI-CNTs-COOH/dopant composite films showed larger currents than the pure PANI film, especially at the peak potentials (see in comparison tables 4-6). This is a demonstration of quicker kinetics in the composite, that can be ascribed to the higher electronic conductivity of the CNTs-CCOH network and the dopants.

Table 4

Electrochemical characteristics of PANI/SWCNTsF modified electrode established from cyclic voltammograms in 0.25 M H₂ SO₄ aqueous solution (monomer free) at 25°C

Cycles	Anodic peaks						Cathodic peaks					
	Ea1, mV	ia1, mA/cm ²	Ea2, mV	ia2, mA/cm ²	Ea3, mV	ia3, mA/cm ²	Ec1, mV	ic1, mA/cm ²	Ec2, mV	ic2, mA/cm ²	Ec3, mV	ic3, mA/cm ²
Cycle 1	257	37.2266	728	26.6016			-1	-27.1094	539	-32.7344		
Cycle 2	275	42.0704	713	25.4297			12	-26.211	540	-31.7579		
Cycle 3	287	41.6016	707	24.8829			18	-25.5079	543	-31.0938		
Cycle 4	290	41.211	533	24.9219			21	-24.7266	534	-30.7812		
Cycle 5	287	41.0546	548	25.3906			24	-24.2187	528	-29.9219		
Cycle 10	305	40.3515	545	25.8985			42	-21.9531	504	-28.2031		
Cycle 20	329	39.2187	533	25.3125			102	-20.1954	456	-25.7031		
Cycle 30	362	38.2031	521	24.961			150	-19.2969	429	-24.4141		
Cycle 40	383	36.836	389	36.7187			165	-18.7891	378	-23.4766		
Cycle 50	401	34.8829	554	22.6173			222	-18.75	333	-22.5		

Table 5

Electrochemical characteristics of PANI/cetyl benzyl dimethyl ammonium chloride /SWCNTsF/ modified electrode established from cyclic voltammograms in 0.25 M H₂ SO₄ aqueous solution (monomer free) at 25°

Cycles	Anodic peaks						Cathodic peaks					
	Ea1, mV	ia1, mA/cm ²	Ea2, mV	ia2, mA/cm ²	Ea3, mV	ia3, mA/cm ²	Ec1, mV	ic1, mA/cm ²	Ec2, mV	ic2, mA/cm ²	Ec3, mV	ic3, mA/cm ²
Cycle 1	416	67.2422					-37	-44.582	446	-41.3632		
Cycle 2	374	60.168					-36	-43.5899	444	-41.1914		
Cycle 3	371	59.7305					-24	-42.8242	444	-40.7774		
Cycle 4	374	59.1758					-18	-42.1289	438	-40.3945		
Cycle 5	377	58.8048	575	45.9531			-12	-41.5274	420	-40.1601		
Cycle 10	377	57.7774	581	46.4687			18	-39.332	321	-40.5507		
Cycle 20	407	57.0625	587	45.418			60	-36.3086	318	-39.3633		
Cycle 30	434	56.168	590	44.3281			90	-34.3437	306	-38.0274		
Cycle 40	458	54.6445					129	-33.3007	288	-36.3476		
Cycle 50	482	52.3945					147	-32.3476	270	-34.2735		

Table 6

Electrochemical characteristics of PANI/KClO₃/SWCNTsF modified electrode established from cyclic voltammograms in 0.25 M H₂ SO₄ aqueous solution (monomer free) at 25°C

Cycles	Anodic peaks						Cathodic peaks					
	Ea1, mV	ia1, mA/cm ²	Ea2, mV	ia2, mA/cm ²	Ea3, mV	ia3, mA/cm ²	Ec1, mV	ic1, mA/cm ²	Ec2, mV	ic2, mA/cm ²	Ec3, mV	ic3, mA/cm ²
Cycle 1	431	38.4375					353	353				
Cycle 2	419	34.2891					348	348				
Cycle 3	419	33.9298					348	348				
Cycle 4	419	33.711					345	345				
Cycle 5	425	33.6211					342	342				
Cycle 10	437	32.7813					321	321				
Cycle 20	467	30.9882					300	300				
Cycle 30	482	29.086					270	270				
Cycle 40	503	27.3476					246	246				
Cycle 50	515	25.5743					240	240				

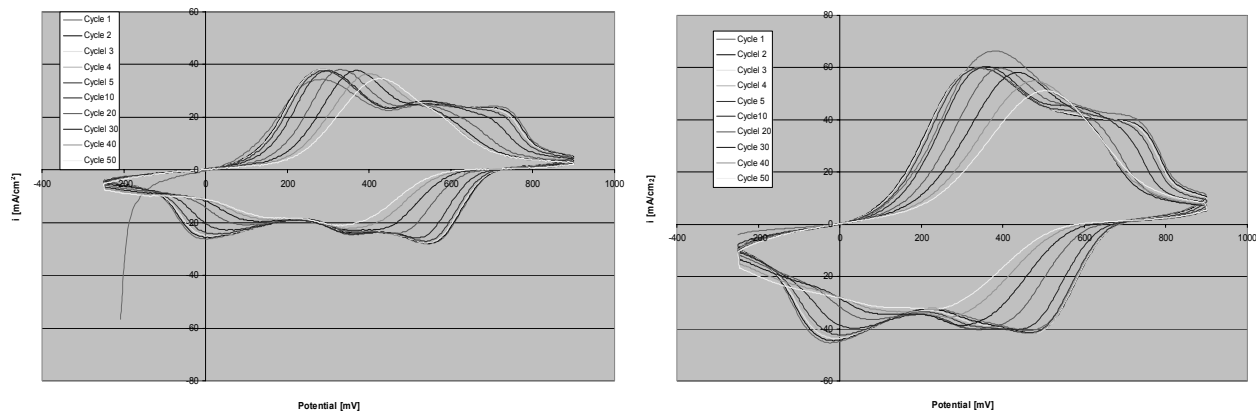


Fig. 4 – Cyclic voltammograms of PANI/ KClO_3/Pt and PANI/ $\text{KClO}_3/\text{SWCNTsF}/\text{Pt}$ composite film in 0.25 M H_2SO_4 cycling solution (monomer free) at 25°C.

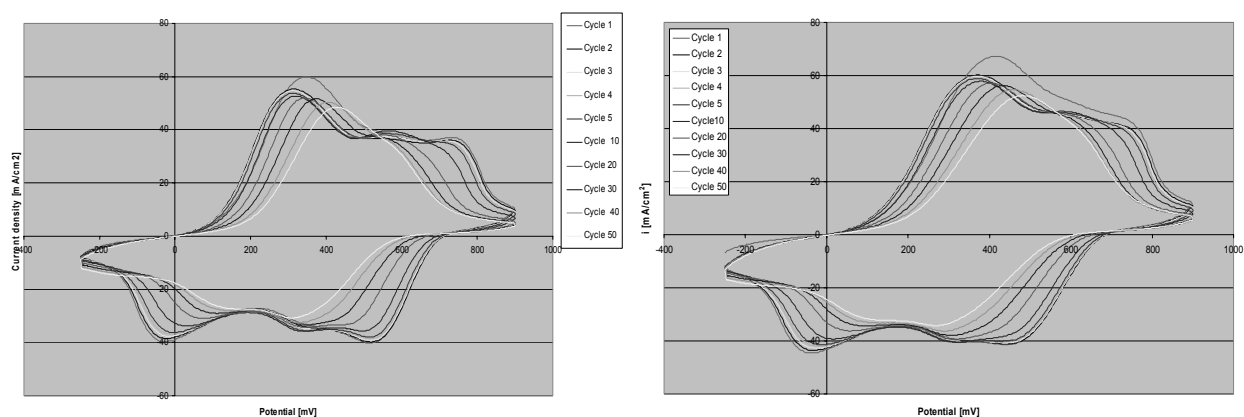


Fig. 5 – Cyclic voltammograms of PANI/ cetyl benzyl dimethyl ammonium chloride/Pt and PANI/ cetyl benzyl dimethyl ammonium chloride /SWCNTsF/Pt composite film in 0.25 M H_2SO_4 cycling solution (monomer free) at 25°C.

The electrochemical activity of PANI/SWCNTs-COOH/Pt, PANI/CDMACI/SWCNTs-COOH/Pt and PANI/ KClO_3 /SWCNTs-COOH/Pt modified electrode in cycling solution is much greater than PANI/Pt in the same cycling solution. In all the cases, in the same circumstances, the PANI/SWCNTs-COOH/Pt, PANI/CDMACI/SWCNTs-COOH/Pt and PANI/ KClO_3 /SWCNTs-COOH/Pt composite film showed anodic peaks much superior and much wider than PANI/Pt film and also, the currents, especially the peak currents much higher. Analyzing in comparison the electrochemical activity of this composite with dopant it can be observed as PANI/CDMACI/SWCNTs-COOH/Pt is much bigger like PANI/ KClO_3 /SWCNTs-COOH/Pt composite film in same condition. The electronic conductivity properties increases in the order: PANI/CDMACI/SWCNTs-COOH/Pt > PANI/SWCNTs-COOH/Pt > PANI/ KClO_3 /SWCNTs-COOH/Pt > PANI/Pt. Consequently, the redox processes that occur in nanocomposite film are more complex and more strong than the ones in the pure PANI film.

Also, the composite layers were analyzed by electrochemical impedance spectroscopy (EIS) at open circuit potential, in an aqueous solution of 0.25 M H_2SO_4 at 25°C. The obtaining Nyquist and Bode diagrams for PANI/Pt, PANI/CNTs-COOH/Pt and PANI/CNTs-COOH/additive/Pt modified electrodes are presented in figures 6-7. The impedance plot is formed of a semicircle at high and middle frequencies and a capacitive slope at low frequencies (see figures 6-7). The semicircle indicated at high frequencies is determined to the charge transfer resistance, which is created at the interface composition between the porous electrode surface and the electrolyte.^{16,17,23-26} At low frequencies, the impedance diagram gets an almost vertical line. The Nyquist plots for PANI/Pt, PANI/CNTs-COOH/Pt and PANI/CNTs-COOH/dopant/Pt composite films are presented by a vertical tendency at low frequencies, showing a capacitive behaviour conformable to the equivalent circuit theory.¹³⁻²² Bode diagrams reveal also the capacitive compartment in conformity with Nyquist plots (see in comparison Figures 6-7).

The capacitances (C) of the electrode materials were estimated, conformable to the equation:

$$C = -1/(2\pi f Z_{im}).$$

(f = frequency; Z_{im} = imaginary impedance), from the slope of the linear correlation between the imaginary impedance and the reciprocal of the frequency at low frequencies.

We can see the 10 times higher capacitance value for PANI/CNTsF and PANI/CNTsF/dopant film in regarding with PANI pure polymeric films (see Table 7). Higher capacitance of the composite films derives clearly from the share of the embedded CNTsF/dopant that ensure interconnected ways for electrons by the CNTsF and ions in the pore network or the direct interaction between the delocalised electrons on polymer chains the CNTsF and the dopant. The real impedance at low frequencies, when the

capacitive compartment controls, is an evidence of the involved resistance of the electrolyte and the film through both electronic and ionic shares. The values of the real impedance at 0.01 Hz are given also in Table 7. It can be observed that the PANI/CNTsF and dopants films have been meaningfully lower in resistance than PANI films. It has been presented that, in the main one the real impedance of a composite film (modified electrode) too decreases as the material's porosity increases because to enhanced ionic accessibility. It can be said that PANI/CNTsF/dopant offered much greater overall conductivity in comparison with the PANI film. As presented that, in general, the real impedance of an electrode material also decreases as the material's porosity increases because of enhanced ionic accessibility.¹⁹⁻²⁵

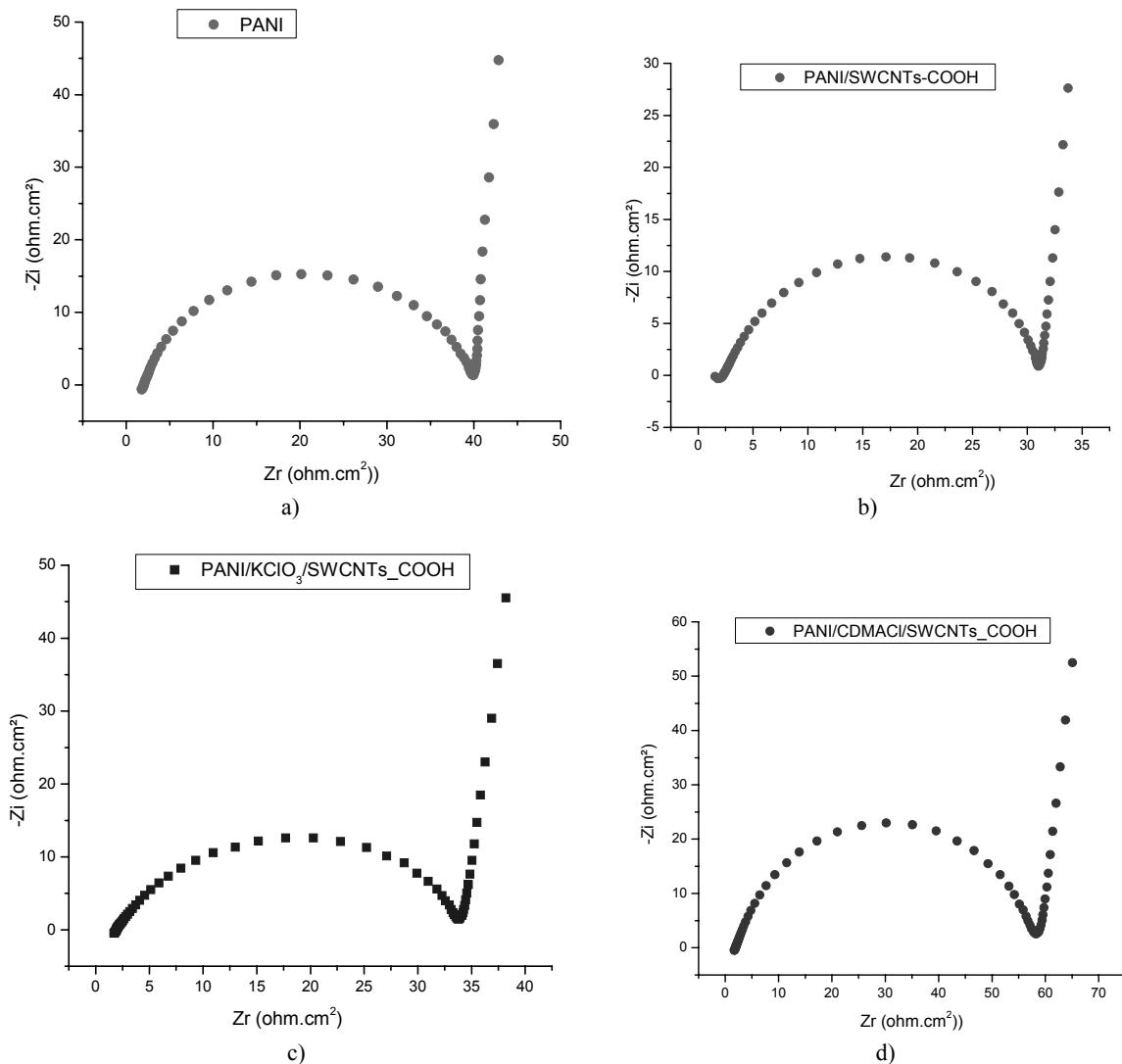


Fig. 6 –The Nyquist diagrams for modified electrodes (a) PANI/Pt; b) PANI/CNTs-COOH/Pt; c) PANI/KClO₃CNTs-COOH/Pt; d) PANI/CBDACl/CNTs-COOH/Pt) at open circuit potential in an aqueous solution of 0.25 M H₂SO₄ and 25°C.

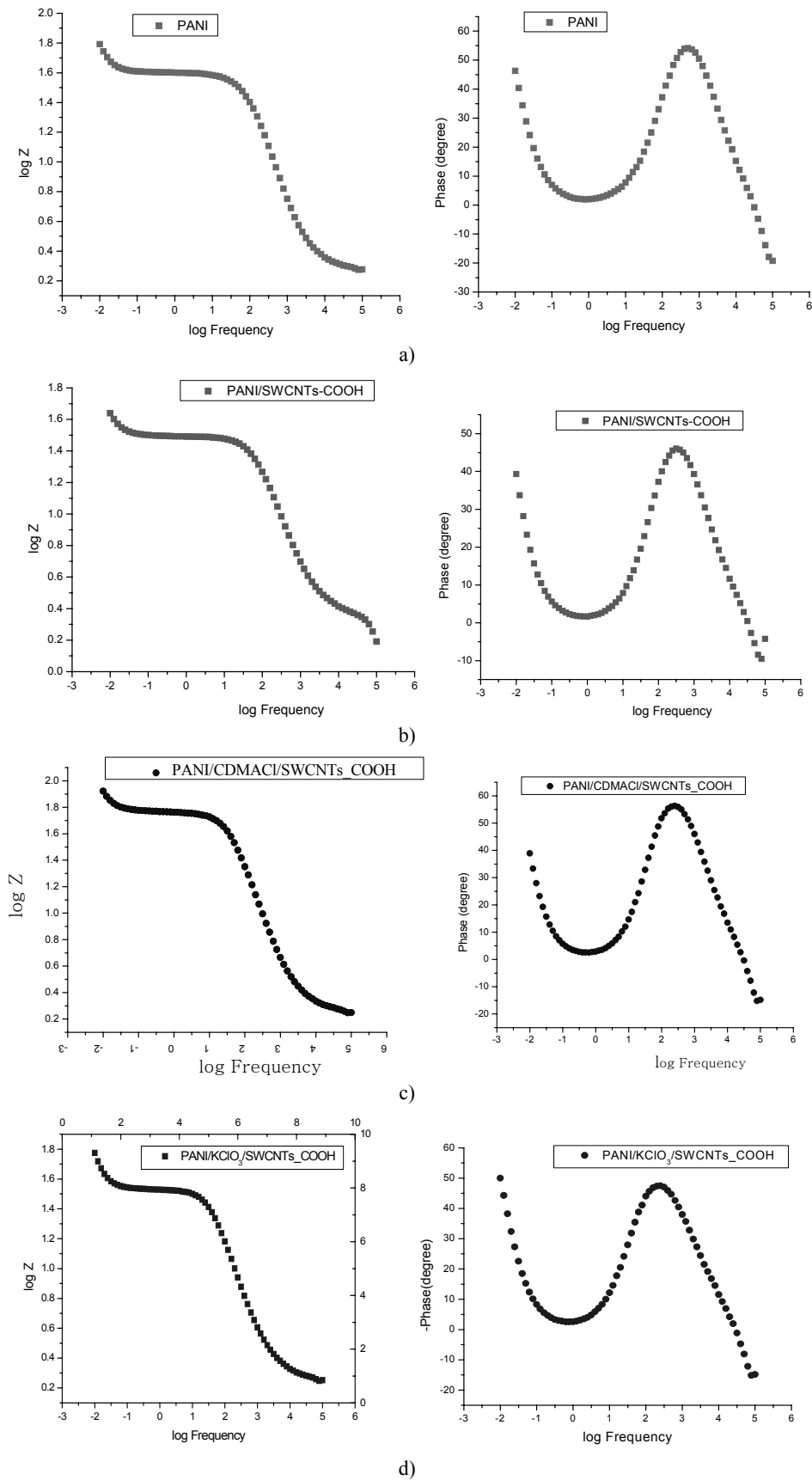


Fig. 7 – The Bode plots for modified electrodes (PANI/Pt, PANI/CNTs-COOH/Pt, PANI/KClO₃/CNTs-COOH/Pt and PANI/CBDACI/CNTs-COOH/Pt) at open circuit potential in an aqueous solution of 0.25M H₂SO₄ and 25°C.

Table 7

Real impedance and capacitance values of pure PANI film and PANI /SWCNTs-COOH nanocomposite film with different dopants obtained by electropolymerization using the cyclic voltammetry (CV) at 0.01Hz

Polymeric film	Slope values obtained From graph: $-Z_{im} = f(1/2\pi f)$	C_{EIS} , F/cm ²	Z_r , Ω cm ²
PANI	42.8	0.023	92.12
PANI/CNTs-COOH	3.68	0.271	58.53
PANI/KClO ₃ /CNTs-COOH	4.25	0.235	78.32
PANI/ cetyl benzyl dimethyl ammonium chloride/CNTs-COOH	2.65	0.378	65.06

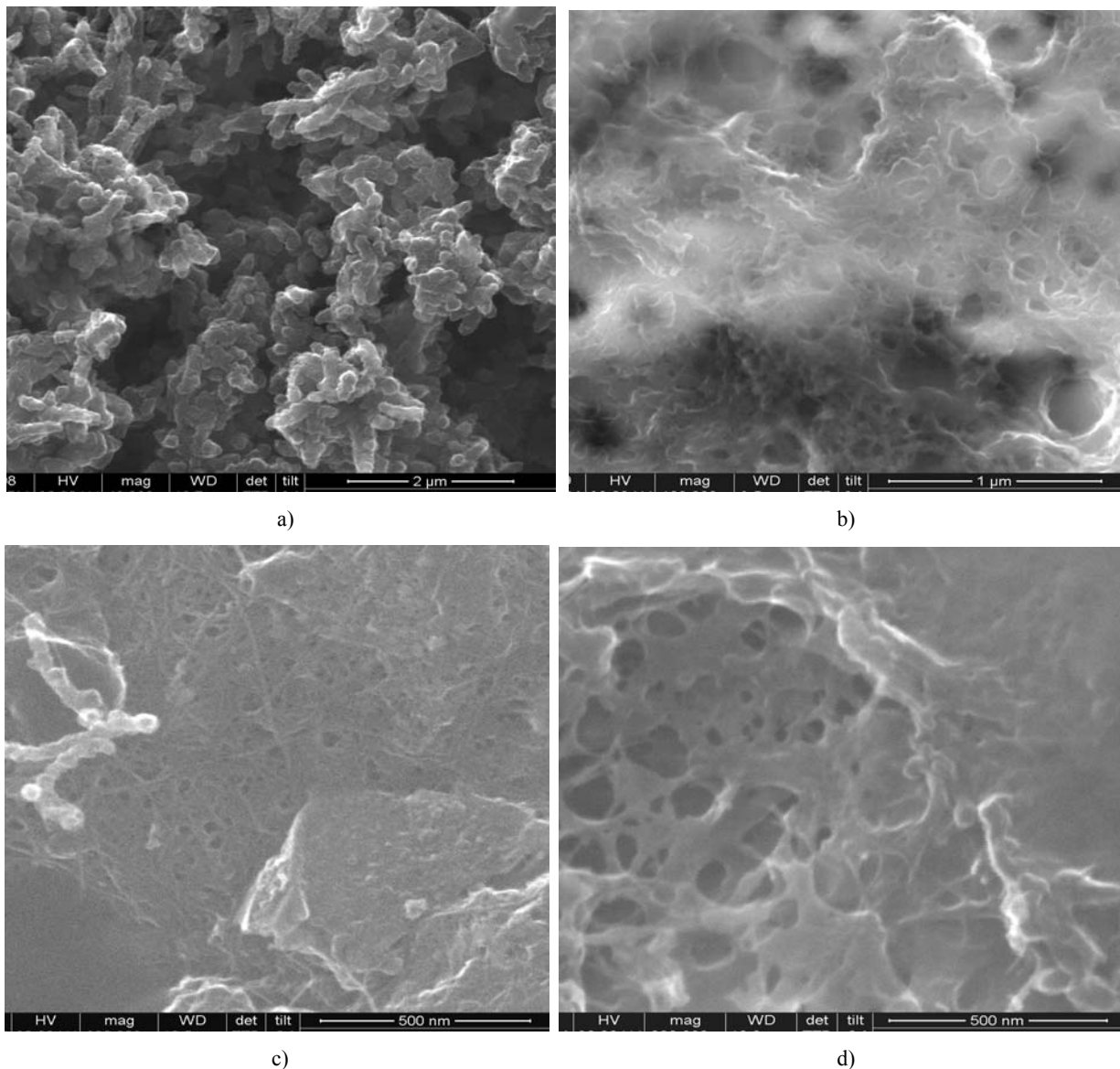


Fig. 8 – SEM images of a) PANI film and b) PANI/CNTs-COOH; c) PANI/KClO₃/CNTs-COOH and d) PANI/CDMACl/CNTs-COOH composite films.

The electrochemical impedance spectroscopy measurements are in concordance with the SEM results exhibited in figure 8 that displayed a

smaller porosity in the PANI film than in the situation of the composite film PANI/CNTs-COOH and PANI/CNTs-COOH/dopant.

In figure 8 are submitted the SEM images of the PANI films, of PANI/CNTs-COOH and of PANI/CNTs-COOH/dopant composite film. This porous morphology enable a superior electrolyte entrance with less resistance by assuring sufficient ways for the displacement of ions and solvent molecules into the composite films that determines to enhanced electrochemical properties. These microstructural shifts have great effect on the capacitive compartment of the composites, as indicated above.

Examining the figures 8 a-d, it can be said that, the PANI and CNTsF/dopant films indicate a morphological structure formation of nanofibers, however for the pure polymeric ones they are little thicker than those in the PANI/CNTsF/dopant composite film. This constitutional similarity can describe the comparatively small difference in electrochemical compartment among PANI, PANI/CNTsF and PANI/CNTsF/dopant as presented previously. Similarly, the morphological structure of the PANI was established to be distinct, the PANI/CNTsF/dopant composite film displaying a more porous morphology. These microstructural transformations have deep effect on the capacitive behavior of the composites, as presented above.

The SEM images showed that the nanocomposite films, PANI/CNTs-COOH and PANI/CNTs-COOH/dopant have been more porous than PANI films (see figure 8a-d). Microstructures of these composites suppose that PANI was wrapped around SWCNTs.

CONCLUSIONS

Were obtained nanocomposite films type PANI/SWCNTs-COOH with cetyl benzyl dimethyl ammonium chloride and KClO_3 as dopants by cyclic voltammetry method from a synthesis solution.

The electrochemical activity of PANI/FSWCNTs/dopant/Pt modified electrode in 0.25 M H_2SO_4 cycling solution is much more higher than of PANI/Pt modified electrode in the same cycling solution;

Electrochemically synthesized composite film of conducting polymer PANI and FSWCNTs-dopant have in common a porous structure at micro-and nano-meter scales.

Cyclic voltammetry (CV) and electrochemical impedance spectroscopy (EIS) demonstrated that these composite films had similar electrochemical

response rates to pure polymeric films but a lower resistance and much improved mechanical integrity.

The electronic conductivity properties increases in the order:

PANI/CDMACI/SWCNTs-COOH/Pt >

PANI/SWCNTs-COOH/Pt >

PANI/ KClO_3 /SWCNTs-COOH/Pt > PANI/Pt.

Nearly rectangular shaped cyclic voltammograms are obtained for all composite films suggesting that the charge and the discharge reversibly occur at the electrode/electrolyte interface.

The best electrochemical properties are presented by PANI/CNTs-COOH/CDMACI/Pt and PANI/CNTs-COOH/Pt.

The Nyquist plots for PANI and composite films PANI/SWCNTs-COOH and PANI/SWCNTs-COOH/dopant are featured by a vertical trend at low frequencies, indicating a capacitive behaviour in concordance to the equivalent circuit theory.

In this study, we have achieved a higher capacitance value for PANI/CNTsF and PANI/CNTsF/dopant film in regarding with PANI pure polymeric films.

The capacitance value increases in the order:

PANI/CDMACI/SWCNTs-COOH/Pt >

PANI/SWCNTs-COOH/Pt >

PANI/ KClO_3 /SWCNTs-COOH/Pt > PANI/Pt

The SEM micrograph of the composite films (PANI/CNTs-COOH and PANI/CNTs-COOH/dopant) shows a porous morphology that wrapped on the surface of FSWCNTs.

The PANI/SWCNTs-COOH/dopant composite is a very important electrode material for employment in the supercapacitor domain.

Acknowledgements: Financial support from PN-II-ID-PCE-2008-2 contract code ID_716, no.596 (The National University Research Council) is gratefully acknowledged.

REFEENCES

1. G. Z. Chen, M. S. P. Shaffer, D. Coleby, G. Dixon, W. Zhou, D. J. Fray and A. H. Windle, *Adv. Mater.*, **2000**, *12*, 522.
2. V. Branzoi, F. Branzoi and A. Musina, *Rev. Roum. Chim.*, **2011**, *56*, 883-893.
3. M. Hughes, G. S. Z. Chen, M. S. Shaffer and A. H. Windle, *Chem. Mater.*, **2002**, *14*, 1640.
4. A. Prună, V. Branzoi and F. Branzoi, *Rev. Roum. Chim.*, **2010**, *55*, 293.
5. V. Branzoi, F. Branzoi and L. Pilan, *Mater. Chem. Phys.*, **2009**, *118*, 197.
6. B. Zhao, H. Hu and R. C. Haddon, *Adv. Funct. Mater.*, **2004**, *14*, 71.

7. P. M. Ajayan, O. Stephan, C. Colliex and D. Trauth, *Science*, **1994**, *265*, 1212.
8. L. Dai and A. W. H. Mau, *Adv. Mater.*, **2001**, *13*, 899.
9. T. Wu, Y-W. Lin and C. S. Liao, *Carbon*, **2005**, *43*, 734.
10. X. Zhang, *Synthetic. Metals.*, **2008**, *158*, 336.
11. Y. Saito, S. Uemura and K. Hamaguchi, *Jpn. J. Appl. Phys.*, **1998**, *37*, L346.
12. E. Bekyarova, M. Davis, T. Burch, M. E. Itkis, B. Zhao, S. Sunshine and R. C. Haddon, *J. Phys. Chem. B*, **2004**, *108*, 19717.
13. H. Hu, Y. Ni, V. Montana, R. C. Haddon and V. Parpura, *Nano Lett.*, **2004**, *4*, 507.
14. T. W. Odom, J. L. Huang, P. Kim and C. M. Lieber, *Nature*, **1998**, *391*, 62.
15. K. Jurewicz, S. Delpeux, V. Bertagna and E. Frackowiak, *Chem Phys. Lett.*, **2001**, *347*, 36.
16. V. Gupta and N. Miura, *Electrochim. Acta*, **2006**, *52*, 1721.
17. Q. Xiao and X. Zhou, *Electrochim. Acta*, **2003**, *48*, 575.
18. J. Zeng, W. Wei, L. Wu, X. Liu, K. Liu and Y. Li, *J. Electroanal. Chem.*, **2006**, *595*, 152.
19. N. Ferrer-Anglada, M. Kaempgen and S. Roth, *Phys. Stat. Sol. B*, **2006**, *243*, 3519.
20. P. Santhosh, K. M. Manesh, K.-P. Lee and A. I. Gopalan, *Electroanalysis*, **2006**, *18*, 894.
21. C. Downs, J. Nugent, P.M. Ajayan and K. S. V. Santhanam, *Adv. Mater*, **1999**, *11*, 1028.
22. C. Peng, J. Jin and G. Z. Chen, *Electrochim. Acta*, **2007**, *53*, 525.
23. J. Wang, J. Dai and T. Yarlagadda, *Langmuir*, **2005**, *21*, 9.
24. Y.C. Tsai, S.C. Li and S.W. Liao, *Biosens and Bioelectron*, **2006**, *22*, 495.
25. V. Branzoi, F. Branzoi, A. Musina and L. Pila, *Rev. Roum. Chim.*, **2011**, *56*, 73-84.
26. F. Branzoi and V. Branzoi, *Int. J. Electrochem. Sci.*, **2016**, *11*, 6564 – 6579.

